Towards direct measurements of remitted photon path lengths in skin: kinetic studies in the range 520-800 nm

V. Lukinsone, M. Osis, J. Latvels, I. Kuzmina, U. Rubins, et al.

V. Lukinsone, M. Osis, J. Latvels, I. Kuzmina, U. Rubins, N. Zorina, A. Maslobojeva, J. Spigulis, "Towards direct measurements of remitted photon path lengths in skin: kinetic studies in the range 520-800 nm," Proc. SPIE 11075, Novel Biophotonics Techniques and Applications V, 1107505 (22 July 2019); doi: 10.1117/12.2526663

SPIE.

Event: European Conferences on Biomedical Optics, 2019, Munich, Germany

Towards direct measurements of remitted photon path lengths in skin: kinetic studies in the spectral range 520-800 nm

V.Lukinsone, M.Osis, J.Latvels, I.Kuzmina, U.Rubins, N.Zorina, A.Maslobojeva, J.Spigulis

Biophotonics Laboratory, Institute of Atomic Physics and Spectroscopy, University of Latvia, Raina Blvd19, Riga, LV-186, Latvia
vanesa.lukinsone@gmail.com

ABSTRACT

Skin-remitted picosecond laser pulses have been detected at variable input-output fiber distances (8 … 20 mm) in the spectral range 520-800 nm, with subsequent analysis of the pulse shape changes. Transfer functions representing the temporal responses of remitted photons to infinitely narrow δ-pulse excitation have been calculated. Parameters related to the photon path length in skin – input-output pulse peak delays, pulse FWHM, travel times of the "initial" photons and distributions of the remitted photon path lengths – are presented and analyzed. The measurement results are in general agreement with the photon propagation model expectations.

Keywords: light propagation in skin, path length of remitted photons, pulsed measurements of skin diffuse reflection, picosecond laser applications.

INTRODUCTION

Light penetration in tissues and the related photon scattering path length are important characteristics in optical diagnostics and therapy. Composition and density of absorbing chromophores influence the scattering path length of diffusely reflected (remitted) photons in various tissues, including human skin. Knowledge on the skin-remitted photon path lengths and their distributions at particular wavelengths is needed for several clinical applications, e.g. for mapping of the chromophore concentration distribution in skin malformations. Theoretical path length estimations can be based on analytic considerations of diffusion theory [1] or numerical Monte Carlo model calculations as presented in our previous study [2]. However, real skin structure at specific body locations may not correspond to the model assumptions and could lead to mistaken results, so direct measurements of remitted photon path length distributions would be preferable.

The skin-remitted laser pulse input-output time delays have been recorded previously in classical double-fiber experiments [3, 4], giving sense about the mean duration of photon travels in skin structures before remission. The photon travel time (or time-of-flight, TOF) is directly related to photon's completed distance in the tissue. Consequently, analysis of the temporal data from pulsed measurements can provide objective information on the photon travel lengths in skin before remission.

In this work, an advanced picosecond laser system for *in vivo* measurements in human skin has been developed and experimentally tested on volunteers. The system allowed changing the wavelength of input pulses and the distance between the emitting and receiving fibers at a constant probe pressure to skin. The remitted pulse parameters at different combinations of wavelengths and the source-detector distances were analyzed.

1. MEASUREMENT SET-UP AND DATA PROCESSING

The developed system is shown schematically in Fig. 1,a. A broadband picosecond laser (*Whitelaser micro supercontinuum lasers, Fianium, NKT PHOTONICS, DK,* pulse full width at half maximum (FWHM) – 6 ps, repetition rate 20 MHz) was used as a light source which emits in the spectral range from 400 nm to 2000 nm. Specific wavelength bands were selected by interference filters. The measurements were taken from the left volar forearms of volunteers aged between 25 and 68 with skin phototypes II and III (Fitzpatrick classification) under permission of the

Novel Biophotonics Techniques and Applications V, edited by Arjen Amelink, Seemantini K. Nadkarni, Proc. of SPIE-OSA
Vol. 11075, 1107505 · © 2019 SPIE-OSA · CCC code: 1605-7422/19/$21 · doi: 10.1117/12.2526663

local Ethics Committee, with written consent of the volunteers. The average spectral power density on skin was ~ 10 mW/cm^2, i.e. well below the skin laser safety limit 200 mW/cm^2 [5].

Two measurement series were performed. In the first one, a set of bandpass optical filters (*Andover Corporation, USA, mod. 550FS10-25, 600FS10-25, 650FS10-25, 700FS10-25, 750FS10-25, 790FS10-25*,) was used with half-bandwidth 10 nm and central wavelengths at 550 nm, 600 nm, 650 nm, 700 nm, 750 nm and 790 nm. For additional spectral filtering, a grating monochromator with resolution 1 nm was used in the detection channel to exclude detection of skin fluorescence signals. Stable recording of optical signals via the input and output fibers (WF-400, *Light Guide Optics International*, LV, silica core diameter 400 microns, length 1,05 m) at various fixed distances between them was ensured by means of a specially designed fiber holding system with inter-fiber distances 8 mm, 12 mm, 16 mm and 20 mm. To provide equal pressure on the skin surface at all measurements, the probe was designed as a lift where the inside sliding part (with selected distances between the two fibers) lies on the skin providing a pressure determined by its weight ~ 35 g/cm^2 (Fig. 1,a – fibers holding system). The outside part of the probe was fixed on the skin during the measurements. Inner forearm skin of 8 volunteers has been examined in the first series.

Photon counting detector (photomultiplier PMC-100-4) combined with the detector controller (DCC-100) and data processing card (SPC-150, all *Becker&Hickl GmbH*, DE) were used for processing of the detected single-photon signals. The data was collected for each selected wavelength by changing the distance between fibers in the skin contact probe as a mean value of 3 successive measurements, each lasting 30 seconds.

The second series of measurements was taken with updated equipment that comprised a set of two equal interference band filters, one of them replacing the monochromator, and a more sensitive photon counting detector (HPM-100-07, *Becker&Hickl GmbH*, DE). The filter set was provided by *Andover Corporation, USA* and included models *520FS10-12.5, 640FS10-12.5, 720FS10-12.5, 800FS10-12.5* with half-bandwidth 10 nm and central wavelengths at 520 nm, 640 nm, 720 nm and 800 nm. This update helped to increase the signal-to-noise ratio and to expand the spectral range of measurements. Inner forearm skin (photo-type II) of 2 volunteers was examined in this series.

Before *in vivo* measurements, the skin input pulse shape (or instrumental response function IRF, Fig.1,b) was recorded by positioning the emitting and receiving fibers face-to-face. It determined the time scale for further measurements. Processing of the measured data involved two steps. First, wavelength-dependences of the time delay between the input-output pulse peak positions and of the full widths at half maximum (FWHM) of the recorded skin-remitted pulses

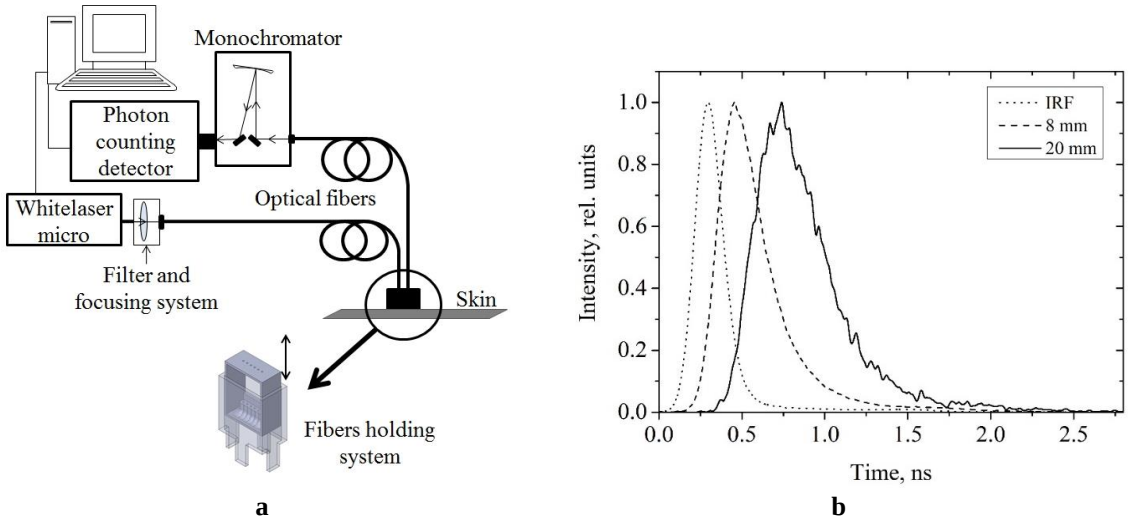

Fig. 1. The set-up for skin remission kinetics measurements (a) and comparison of the 650 nm IRF pulse with skin-remitted pulses at two inter-fiber distances (b).

at all inter-fiber distances were analyzed. A special program for signal processing was created in *MatLab*. The differences of both parameters with respect to the IRF pulse were calculated. The measurement error was estimated by summing the measurement setup error (approximately 6 ps) and quadratic deviation of the average measurement value.

At the second step, distributions of the skin-remitted photon path lengths were sought by comparing the shapes of skin input and output pulses (*a(t)* and *b(t)*, respectively). The temporal distribution function *f(t)* of photon arrivals could be measured directly if infinitely narrow δ-pulse of input photons would be launched into skin. As laser pulses with tens of picoseconds duration (at half-maximum) were used in our experiments, the skin-remitted pulses were temporally shifted and broadened:

$$b(t) = \int_0^t a(t-\tau) f(\tau) d\tau \qquad (1).$$

This ill-posed inverse problem – to find the distribution function *f(t)* - was solved by the Tikhonov regularization method [6, 7]. After restoring *f(t)*, the corresponding distribution of back-scattered photon path lengths was calculated as

$$\phi(s) = f(t) \cdot c/n \qquad (2),$$

where *c* is the speed of light in vacuum and *n* is the mean refraction index of superficial skin tissues (n ~ 1.4 [8]).

2. RESULTS

Figure 2 illustrates the results of input and output pulse parameters obtained in the 1st measurement series – dependencies of the pulse peak time delays (MAX) and differences of the pulse FWHM values on the distance between input and output fibers at all exploited spectral bands, averaged over 8 volunteers. As expected, increased inter-fiber distance has led to increased time delay between the input and output pulse peaks and broadening of the remitted pulses in the spectral range 550-790 nm.

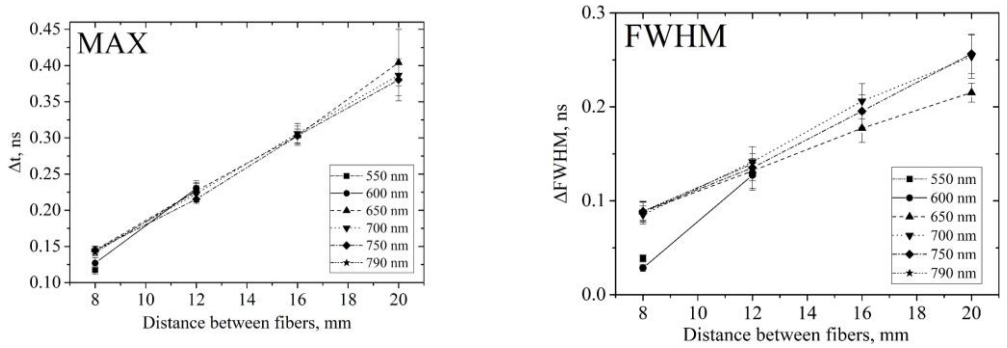

Fig. 2. Dependences of the mean values of pulse peak time delay (a) and FWHM differences (b) on inter-fiber distances at six illumination wavelengths.

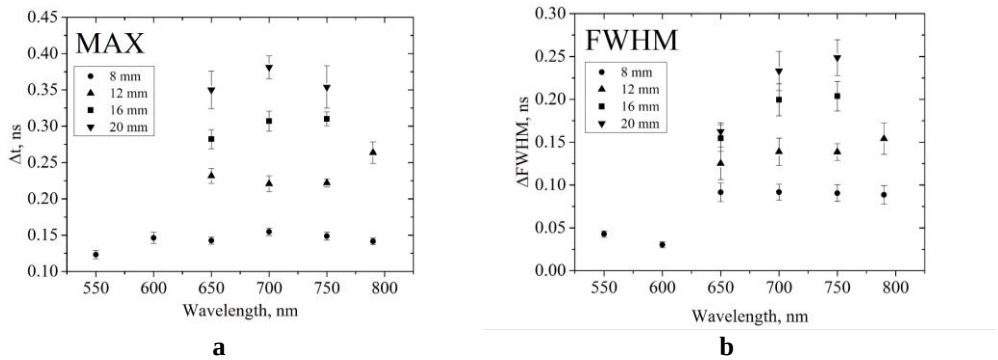

Fig. 3. Spectral dependences of the pulse peak time delay (a) and the FWHM differences (b) at four inter-fiber distances for a single volunteer.

We assumed that the values of MAX and FWHM would notably increase at wavelengths longer than 600 nm where hemoglobin absorption significantly decreases [9]. Data from a single volunteer showed the expected increase at inter-fiber distance 8 mm (Figure 3); at longer distances remitted photon signals of the 550 nm and 600 nm bands were extremely weak, undistinguishable from the noise level.

The shortest photon path length in skin was calculated from the measured time delay between the "initial" moments related to 10% level of the pulse maximum at the raising fronts of the IRF and skin-remitted pulses, respectively. Figure 4 illustrates the obtained spectral dependence of the "initial" photon path lengths for the inter-fiber distance 8 mm. At longer inter-fiber distances, the shortest photon path lengths increased for about 2.5 times.

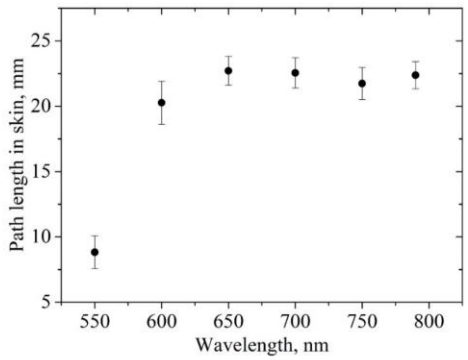

Fig. 4. Path lengths of the "initial" backscattered photons for six wavelength bands at 8mm inter-fiber distance (a single volunteer).

A result of the 2nd measurement series – comparison of the IRF and remitted light pulse shapes for the 520 nm and 800 nm band at various inter-fiber distances – is illustrated in Figure 5. The signal-to-noise ratio in this series was much better; it helped to detect signals also at a shorter wavelength 520 nm.

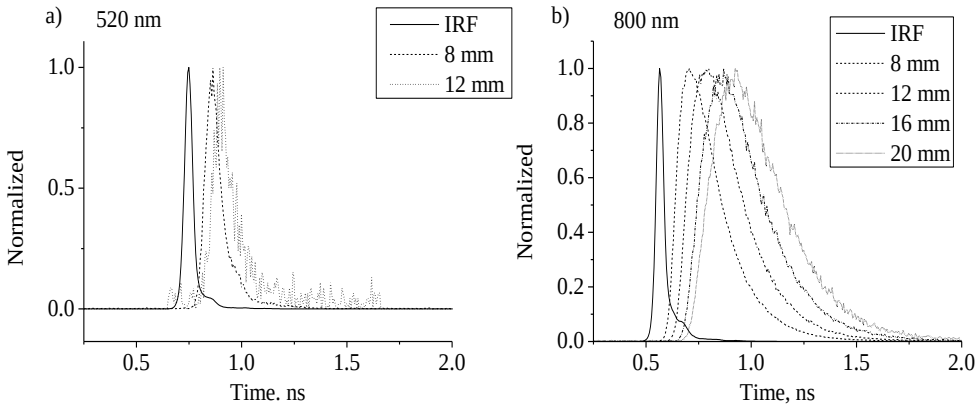

Fig. 5. The 520 nm (a) and 800 nm (b) input and output pulse shapes at various inter-fiber distances (a single volunteer, the 2nd measurement series).

The 2nd series measurement data are collected in Table 1. The changes of MAX and HWFM values showed similar temporal tendencies as in the 1st series (Figs. 2,3). In addition, one more parameter – the "longest" photon path length in skin L was calculated (2) with the measured time intervals between the input pulse peak positions and the time points corresponding to 2% level of the remitted pulse at its falling front. It has varied in a very broad range, from 11.7 cm to more than 30 cm.

Table 1. The measured skin-remitted pulse parameters (2nd series)

λ, nm	MAX, ns (±0.012)				Δ FWHM, ns (±0.02)				L, mm (±12)			
	8 mm	12 mm	16 mm	20 mm	8 mm	12 mm	16 mm	20 mm	8 mm	12 mm	16 mm	20 mm
520	0.114	0.168	0.173	-	0.086	0.106	-	-	117	105	-	-
640	0.103	0.222	0.304	0.315	0.155	0.228	0.319	0.319	162	204	268	276
720	0.114	0.211	0.282	0.353	0.205	0.273	0.318	0.367	273	266	267	308
800	0.141	0.234	0.304	0.369	0.227	0.279	0.325	0.376	251	300	319	304

Finally, skin-remitted photon path length distributions were determined accordingly to (1) and (2) for the four selected wavelength bands (Fig. 6). The inverse problem solving proved to be very sensitive to fluctuations of the measured pulsed signals – it was most pronounced in the case of 640 nm wavelength band. Some oscillations in the restored functions are present, especially in the tail region of 520 nm band. The smoothest photon path length distributions were obtained for the 720 nm band.

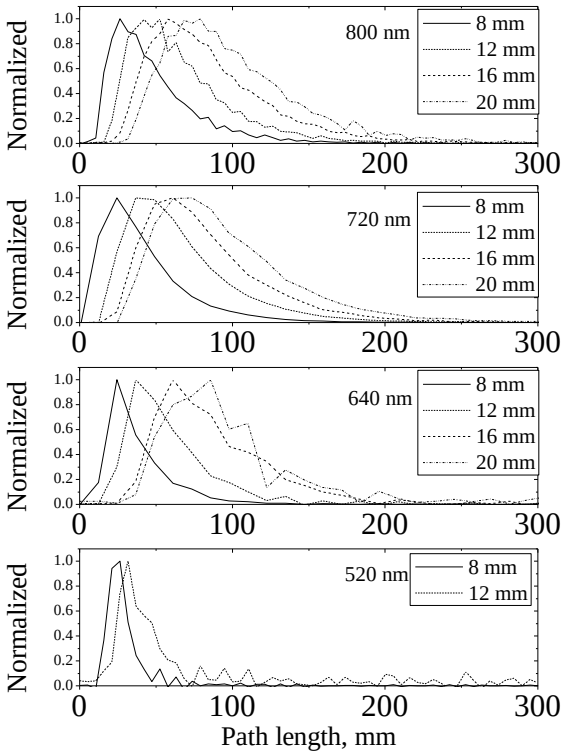

Fig.6. The skin-remitted photon path length distributions, calculated accordingly to (1) and (2) with the pulse measurement data.

3. DISCUSSION

The obtained results are in general agreement with the diffusion theory for photon propagation in turbid media. Photon path lengths in skin critically depend on the chromophore absorption at particular wavelengths. For instance, the spectral dependence of the path lengths of skin-remitted "initial" photons (Fig. 4) correlates to blood hemoglobin absorption. The absorption of hemoglobin is much higher at 550 nm than in the 600-790 nm range [9], therefore the detected signals at 550 nm were very weak and only few photons with "ballistic" trajectories could be registered. Meanwhile, for 650 nm and longer wavelengths less photons were lost, so in result of scattering they could travel via deeper skin layers with correspondingly longer path lengths. Hemoglobin absorption in this spectral range radically decreases but that of water and lipids increases – this may explain why the travel times and the corresponding path lengths of the "initial" remitted photons in the 650-790 nm range appear to be nearly the same. Similar trend was

observed regarding the "longest" path lengths of photons in skin (L, Table 1), as well as by comparing the skin-remitted pulse shapes at 520 nm and 800 nm (Fig. 5).

To the best of our knowledge, no experimental data on the distributions of skin-remitted photon path lengths at different wavelengths have been available before this study. The results presented at Fig. 6 show that distributions in the 720-800 nm spectral range (low hemoglobin absorption) are fairly similar, while those at 520 nm (high hemoglobin absorption) are much "narrower". The peak values of the distributions, depending on the input-output distance, are positioned in the range of 20-100 mm for the 640-800 nm spectral interval and in the range of 20-40 nm for the 520 nm band. The presented distributions can be used for estimation of the mean path length of remitted photons in forearm skin at each particular wavelength-distance combination which may be helpful for skin chromophore mapping and other applications. Results of the very first deconvolution attempts by the Tikhonov's regularization method have clearly demonstrated its potential. However, more efforts are to be put in future both in hardware and software developments in order to get more precise data on the photon path length distributions in skin tissues.

4. SUMMARY

To conclude, new experimental data on photon propagation times and path lengths in human skin have been obtained in this study by means of picosecond-range optical pulse measurements on volunteers. The presented results encourage continuing this research, in future focusing on improvements of the experimental setup (in order to achieve higher sensitivity and temporal resolution), as well as on the data processing technology - especially with respect to the deconvolution calculations that allow gaining more information on the distributions of the photon path lengths in human skin for diagnostic and therapeutic applications.

ACKNOWLEDGEMENTS

This work was supported by the ERDF project #1.1.1.1/18/A/132 and the Laserlab-Europe project #EU-H2020 654148.

REFERENCES

[1] D.J.Faber, N. van Sterkenburg, A.L.Post, T.G. van Leeuwen, "Pathlength distribution of (sub)diffusively reflected light", *Proc. SPIE* **10876**, 1087608 (2019).
[2] J.Spigulis, I.Oshina, A.Berzina, A.Bykov, "Smartphone snapshot mapping of skin chromophores under triple-wavelength laser illumination", J. *Biomed. Opt.* **22**(9), 091508 (2017).
[3] J.-C.Bernengo, H.Adhoute, D.Mougin, "Measurement of the time of flight of photons into the skin: influence of site, age and gender, correlation with other skin parameters", *Skin Res. Techn.* **21**(1), 25-34 (2015).
[4] A.Dzerve, I.Ferulova, A.Lihachev, J.Spigulis, "Time of flight for photon in human skin", *J.Biomed.Phot.&Eng.* **2**(3), 030301-1-4 (2016).
[5] *Safety of Laser Products* - Part 1: Equipment Classification and Requirements IEC 60825-1, 2007
[6] G.Revalde, N.Zorina, A.Skudra, Z.Gavare, "Deconvolution of the line spectra of microsize light sources in the magnetic field", *Rom.Rep.Phys.* **66**(4), 1099–1109 (2014).
[7] G.Revalde, N.Zorina, A.Skudra, "Multicomponent line profile restoring by means of ill-posed inverse task solution", *J.Phys.: Conf.Series*, **810**(1), 012056 (2017).
[8] H.Ding, J.Q.Lu , W.A.Wooden, P.J. Kragel, X-H.Hu, "Refractive indices of human skin tissues at eight wavelengths and estimated dispersion relations between 300 and 1600 nm" *Phys. Med. Biol.* **51,** 1479–1489 (2006).
[9] "Optical absorption of hemoglobin" (online): Oregon Med. Laser Center, https://omlc.org/spectra/hemoglobin/ (2017).